Computers and Concrete, Vol. 6, No. 5 (2009) 357-376 357
DOI: http://dx.doi.org/10.12989/cac.2009.6.5.357

Maximum axial load level and minimum confinement for limited ductility design of high-strength concrete columns

J. Y. K. Lam†, J. C. M. Ho‡ and A. K. H. Kwan‡†

Department of Civil Engineering, The University of Hong Kong, Pokfulam, Hong Kong

(Received January 5, 2009, Accepted July 30, 2009)

Abstract In the design of concrete columns, it is important to provide some nominal flexural ductility even for structures not subjected to earthquake attack. Currently, the nominal flexural ductility is provided by imposing empirical deemed-to-satisfy rules, which limit the minimum size and maximum spacing of the confining reinforcement. However, these existing empirical rules have the major shortcoming that the actual level of flexural ductility provided is not consistent, being generally lower at higher concrete strength or higher axial load level. Hence, for high-strength concrete columns subjected to high axial loads, these existing rules are unsafe. Herein, the combined effects of concrete strength, axial load level, confining pressure and longitudinal steel ratio on the flexural ductility are evaluated using nonlinear moment-curvature analysis. Based on the numerical results, a new design method that provides a consistent level of nominal flexural ductility by imposing an upper limit to the axial load level or a lower limit to the confining pressure is developed. Lastly, two formulas and one design chart for direct evaluation of the maximum axial load level and minimum confining pressure are produced.

Keywords: columns; confinement; ductility; high-strength concrete.

1. Introduction

When designing reinforced concrete columns, most structural engineers just concentrate on the provision of sufficient strength to resist the vertical and lateral loads at ultimate limit state and sufficient stiffness to limit the column drift at serviceability limit state. Although it is well known that from the structural safety point of view, ductility is at least as important as strength (Bechtoula H. 2005, Chung *et al.* 2004, Wu *et al.* 2004, Chung *et al.* 2006, Kim 2005, Kim and Kim 2007, Kim *et al.* 2008, Maghsoudi and Bengar 2006, Marefat *et al.* 2005, Rubinstein *et al.* 2007), only nominal ductility is provided by following empirical deemed-to-satisfy rules, e.g., limitations on minimum bar size and maximum spacing, for detailing of the confining reinforcement. Decades of practice have demonstrated that for normal-strength concrete (NSC) columns not subjected to impact or earthquake loads, these empirical rules are generally satisfactory in the provision of sufficient ductility. However, in recent years, it has been found from experimental investigations (Bayrak and Sheikh 1998, Kim and Kim 2007, Li *et al.* 1991, Maghsoudi and Bengar 2006, Mendis

† Ph. D. Student
‡ Assistant Professor, Corresponding author, E-mail: johnny.ho@hku.hk
‡† Professor

et al. 2000, Razvi and Saatcioglu 1994, Sheikh *et al.* 1994) that the ductility so provided by following these empirical rules decreases as the concrete strength increases and that therefore, for high-strength concrete (HSC) columns, a larger amount of confining reinforcement is needed to provide the same ductility as has been provided in the past to NSC columns. Furthermore, it has been shown by both theoretical (Au and Bai 2006, Carreira and Chu 1986, Fafitis and Shah 1985, Kim 2005, Sung *et al.* 2005, Lu and Zhou 2007) and experimental (Bayrak and Sheikh 1997, Bechtoula *et al.* 2005, Chung *et al.* 2004, Marefat *et al.* 2005, Rubinstein *et al.* 2007, Watson and Park 1994) studies that the ductility also decreases as the axial load level increases.

From the above, it is evident that the existing empirical rules stipulated in the design codes do not provide a consistent level of nominal ductility and may even be unsafe when applied to HSC columns. For an overview, a summary of some existing rules is given in the following, where d_b= diameter of longitudinal reinforcement; d_s=diameter of confining reinforcement; s=spacing of confining reinforcement; h=overall depth of column section and ρ=longitudinal steel ratio:

(1) American ACI 318-05 (ACI Committee 318 2005): $d_s \geq 10$ mm for $d_b \leq 32$ mm; $d_s \geq 13$ mm for $d_b > 32$ mm; $s \leq 16d_b$ or $48d_s$ or h whichever is the smallest.
(2) Australian AS 3600-2001 (Standard Australia 2001): $d_s \geq 6$ mm for $d_b < 20$ mm; $d_s \geq 10$ mm for $d_b \geq 20$ mm; $s \leq 15d_b$ or h whichever is the smaller.
(3) European EC 2-2004 (European Committee for Standardization 2004): $d_s \geq 6$ mm or $0.25d_b$ whichever is the larger; $s \leq 20d_b$ or h or 400 mm whichever is the smallest.
(4) Chinese GB 50010-2002 (Ministry of Construction 2002): $d_s \geq 6$ mm or $0.25d_b$ whichever is the larger for $\rho \leq 3\%$; $d_s \geq 8$ mm or $0.25d_b$ whichever is the larger for $\rho > 3\%$; $s \leq 15d_b$ or h or 400 mm whichever is the smallest for $\rho \leq 3\%$; $s \leq 10d_b$ or 200 mm whichever is the smaller for $\rho > 3\%$.
(5) Hong Kong Concrete Code 2004 (Buildings Department 2004): $d_s \geq 6$ mm or $0.25d_b$ whichever is the larger; $s \leq 12d_b$ or h whichever is the smaller.

Although the above empirical rules for detailing of the confining reinforcement appear to be quite different in the different design codes, the actual confining pressures provided are more or less the same. Using the formula developed by Mander *et al.* (1988), the minimum confining pressure provided in each design code has been evaluated based on longitudinal steel diameter larger than 20 mm, as listed in Table 1. This is understandable because according to the design principle of strong column and weak beam, plastic hinges should only appear at the base of the lowest storey columns in multi-storey buildings, where the longitudinal steel content is fairly large in order to sustain the axial load from upper storeys. From this table, it can be seen that the minimum confining pressures

Table 1 Nominal flexural ductility provided in existing design codes

Design code	Minimum confining pressure (MPa)	Curvature ductility factor μ			
		f_{co} = 20 MPa		f_{co} = 40 MPa	
		P/A_gf_{co} = 0.2	P/A_gf_{co} = 0.4	P/A_gf_{co} = 0.2	P/A_gf_{co} = 0.4
American ACI 318	0.24	6.00	4.86	4.71	2.87
Australian AS 3600	0.24	6.00	4.86	4.71	2.87
European EC 2	0.18	5.62	4.51	4.46	2.73
Chinese GB 50010	0.18	5.62	4.51	4.46	2.73
Hong Kong Concrete Code	0.19	5.68	4.57	4.50	2.76

provided in the design codes vary within the narrow range of 0.18 to 0.24 MPa. With such minimum confining pressures provided, the flexural ductility achieved within the range of concrete strength of f_{co}=20 to 40 MPa and the range of axial load level of $P/A_g f_{co}$=0.2 to 0.4 (f_{co} is the uniaxial compressive strength of the concrete, P is the axial load applied and A_g is the area of the concrete section) has been evaluated using nonlinear moment-curvature analysis as per the method recently developed by the authors (Au and Bai 2006, Au and Kwan 2004, Au *et al.* 2005, Ho *et al.* 2004, Kwan *et al.* 2002, Kwan *et al.* 2004). The flexural ductility so evaluated is expressed in terms of the curvature ductility factor μ defined by Park and Paulay (1975), which has also been adopted by others (Au and Kwan 2004, Au *et al.* 2005, Galal 2007, Maghsoudi and Bengar 2006, Rubinstein *et al.* 2007). The results for the various design codes are presented in the third to sixth columns of Table 1. It should be noted that the curvature ductility factors adopted in this study refer to the section ductility, which can be related to the member's ductility (e.g. displacement ductility and rotation ductility) through the "plastic hinge length".

From these results, it is clear that the curvature ductility factor decreases as the concrete strength f_{co} or the axial load level $P/A_g f_{co}$ increases. Nevertheless, provided that the concrete strength f_{co} is not higher than 40 MPa and the axial load level $P/A_g f_{co}$ is not higher than 0.4, a certain minimum curvature ductility factor $\mu_{\min}$ is provided by each design code. Referring to the last column of Table 1, it can be seen that the minimum curvature ductility factors provided by the various codes vary from 2.73 to 2.87. On average, for NSC columns, the minimum curvature ductility factor being provided as nominal ductility by the existing codes is about 2.80. In a previous study by the authors (Au and Kwan 2004, Ho *et al.* 2004), it has been found that for NSC beams, the minimum curvature ductility factor being provided as nominal ductility by the existing codes is 3.32. Hence, the minimum curvature ductility factors being provided to NSC columns and NSC beams are not too different from each other. For consistency and simplicity, it is proposed to adopt a single value of $\mu_{\min}$=3.32 for both columns and beams.

With a view to improving the ductility design of NSC and HSC columns so as to ensure the provision of a consistent level of nominal ductility, it is advocated herein that the traditional practice of imposing empirical deemed-to-satisfy detailing rules should be abandoned and replaced by a more scientific approach of imposing a fixed minimum curvature ductility factor $\mu_{\min}$ as a nominal requirement. For structures not subjected to impact or earthquake loads, the value of $\mu_{\min}$ may be taken as 3.32 while for structures subjected to impact or earthquake loads, a higher value should be adopted, depending on the actual ductility demand.

In the present study, the combined effects of concrete strength, axial load level, confining pressure and longitudinal steel ratio on the flexural ductility of concrete columns are evaluated using nonlinear moment-curvature analysis. It will be shown towards the end of the study that in order to achieve the required minimum curvature ductility factor $\mu_{\min}$, there is a necessity of imposing a limit on either the maximum axial load level or the minimum confining pressure. The allowable maximum axial load level is dependent on the confining pressure provided while the required minimum confining pressure is dependent on the axial load level applied. Hence, no fixed limits could be imposed. Nevertheless, two formulas and one design chart have been produced for direct evaluation of the maximum axial load and minimum confining pressure.

2. Nonlinear moment-curvature analysis

The method of analysis employed herein has been presented before in a series of studies conducted by the authors (Au and Kwan 2004, Au *et al.* 2005, Ho *et al.* 2004, Kwan *et al.* 2002, Kwan *et al.* 2004). It takes into account the actual stress-strain curves of the constitutive materials as well as the stress-path dependence of the longitudinal steel reinforcement.

For the concrete, the stress-strain curves developed by Attard and Setunge (1996) for unconfined and confined concrete, which have been shown to be applicable to a broad range of in-situ uniaxial concrete strength f_{co} from 20 to 130 MPa, are adopted. Fig. 1(a) shows the typical stress-strain curves of concrete subjected to different confining pressures.

For the steel reinforcement, a linearly elastic-perfectly plastic stress-strain curve is adopted. Since there could be strain increment reversal in the steel reinforcement despite monotonic increase of curvature during failure, the stress-strain curve of the steel reinforcement is stress-path dependent. The unloading path of the stress-strain curve is assumed to follow the same slope as the initial elastic portion of the stress-strain curve. Strain hardening of the steel has not been incorporated as it has been found that the effect of strain hardening is generally insignificant except when the steel content of the section is very low (Ho *et al.* 2005). Fig. 1(b) shows the stress-strain curve of the steel reinforcement with stress-path dependence considered.

In the analysis, the axial load is applied at the geometric centre of the column section at the beginning before any curvature or moment is applied. The moment-curvature behaviour of the column section is then analysed by applying prescribed curvatures to the section incrementally starting from zero. At a given curvature, the stresses developed in the core concrete (assumed to be confined), cover concrete (assumed to be unconfined) and longitudinal steel are determined from the strain profile and their respective stress-strain curves. The neutral axis depth and resisting moment are subsequently evaluated from the conditions of axial and moment equilibrium. The above procedure is repeated until the curvature is large enough for the resisting moment to increase to the peak and then decrease to 50% of the peak moment.

Based on the moment-curvature analysis, a parametric study on the flexural ductility of column sections has been carried out. The column sections analysed are shown in Fig. 2. They are all 1.0 m by 1.0 m square column sections, each with longitudinal steel reinforcement placed uniformly around the perimeter. In order to cover both NSC and HSC in the parametric study, the concrete

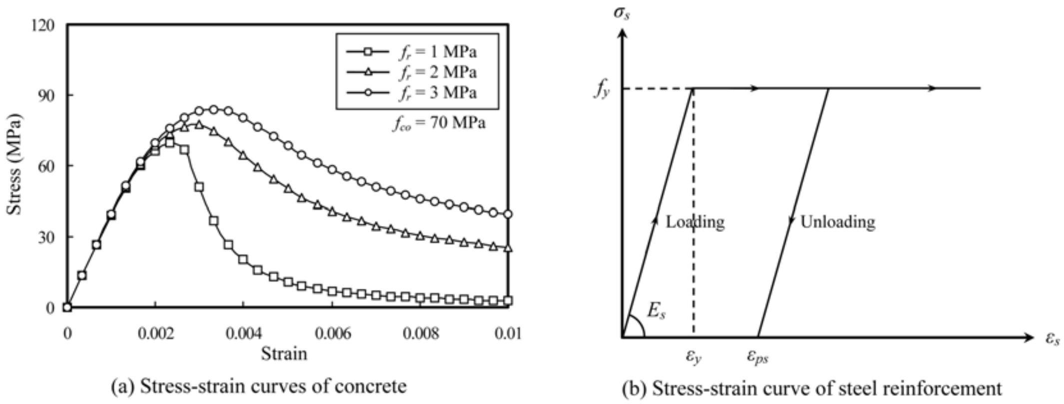

Fig. 1 Stress-strain curves of concrete and steel reinforcement

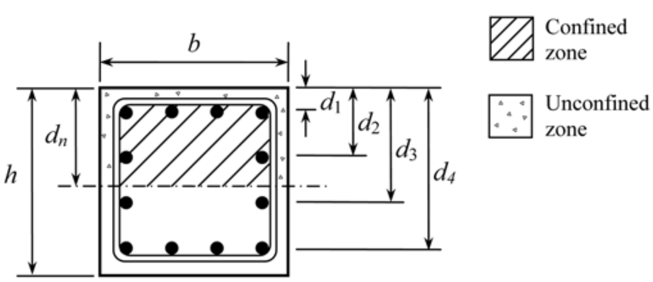

<u>Section properties</u>

- $b = h = 1000$ mm
- $A_g = bh = 1.0$ m^2
- $d_1 = 80$ mm
- $d_2 = 360$ mm
- $d_3 = 640$ mm
- $d_4 = 920$ mm
- $f_{co} = 40$ to 100 MPa
- $f_y = 460$ MPa
- $f_r = 0$ to 4 MPa
- $P/A_g f_{co} = 0.1$ to 0.6
- $\rho = A_s/A_g = 1$ to 6 %

Fig. 2 Column sections analysed

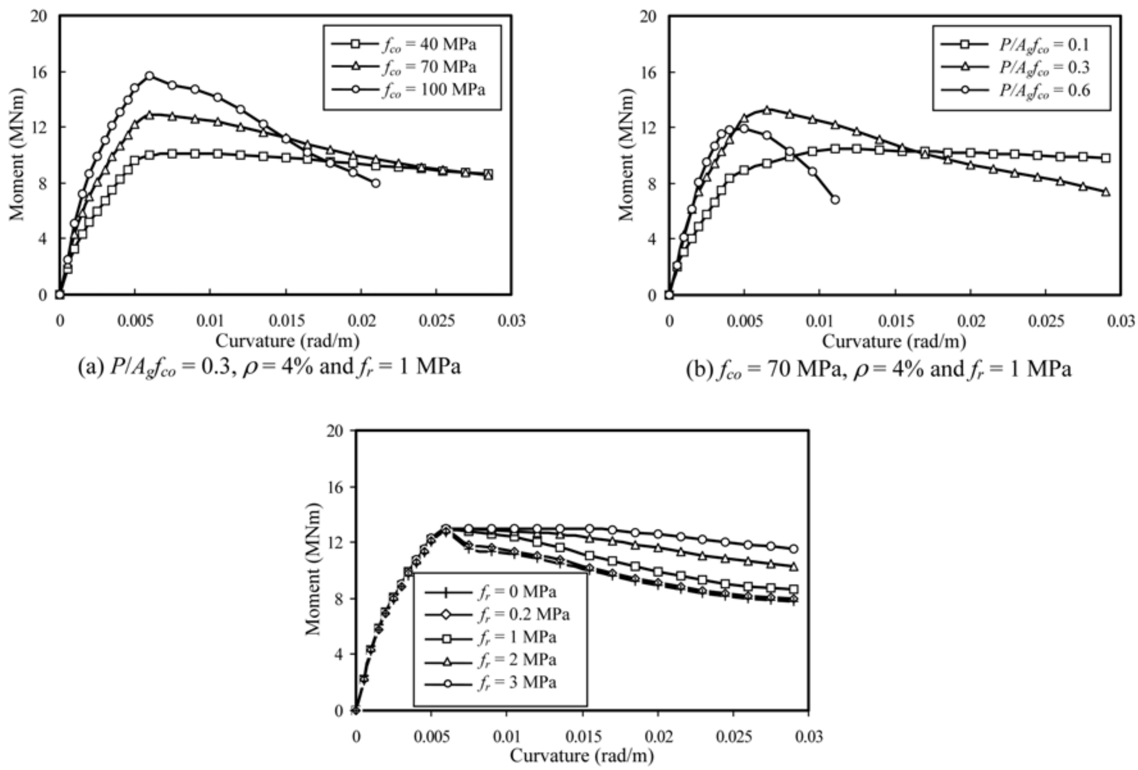

(a) $P/A_g f_{co} = 0.3$, $\rho = 4\%$ and $f_r = 1$ MPa

(b) $f_{co} = 70$ MPa, $\rho = 4\%$ and $f_r = 1$ MPa

(c) $f_{co} = 70$ MPa, $P/A_g f_{co} = 0.3$ and $\rho = 4\%$

Fig. 3 Moment-curvature curves of column sections strength f_{co} is varied from 40 to 100 MPa. Furthermore, the axial load level $P/A_g f_{co}$ is varied from 0.1 to 0.6, the confining pressure f_r is varied from 0 to 4 MPa, and the longitudinal steel ratio ρ is varied from 1 to 6% to study their effects. A constant steel yield strength of f_y=460 MPa is adopted in the parametric study.

Some of the moment-curvature curves obtained are plotted in Fig. 3. Fig. 3(a) shows the moment-curvature curves at a constant axial load level of $P/A_g f_{co}$=0.3 and various concrete strengths of f_{co}= 40, 70 and 100 MPa. It can be seen from these curves that as the concrete strength increases, the flexural strength increases but the flexural ductility decreases. Fig. 3(b) shows the moment-curvature curves at a constant concrete strength of f_{co}=70 MPa and various axial load levels of $P/A_g f_{co}$=0.1, 0.3 and 0.6. It can be seen from these curves that as the axial load level increases from 0.1 to 0.3, the flexural strength increases but as the axial load level further increases from 0.3 to 0.6, the flexural strength decreases. On the other hand, as the axial load level increases, the flexural ductility always decreases. Fig. 3(c) shows the moment-curvature curves at a constant concrete strength of f_{co} =70 MPa, a constant axial load level of $P/A_g f_{co}$=0.3 and various confining pressures of f_r=0, 0.2, 1, 2 and 3 MPa. The moment-curvature curves for f_r=0 and 0.2 MPa refer to the unconfined column section and column section containing minimum confining pressure designed according to some of the existing codes (ACI Committee 318 2005, Buildings Department 2004, European Committee for Standardization 2004, Ministry of Construction 2002, Standard Australia 2001). It is evident from these curves that as the confining pressure increases, the flexural strength increases marginally while the flexural ductility increases considerably. In other words, the provision of confining pressure would not significantly increase the flexural strength but is an effective means of improving the flexural ductility.

3. Balanced axial load level and minimum flexural ductility

3.1 Failure modes and balanced axial load level

Three failure modes are observed. They are: (1) tension failure, in which the maximum strain that can be developed in tension steel under flexure is larger than its yield strain; (2) compression failure, in which the maximum strain that can be developed in tension steel under flexure is smaller than its yield strain; and (3) balanced failure, in which the maximum strain that can be developed in tension steel under flexure is equal to its yield strain. Tension failure occurs in columns subjected to a relatively low axial load level and/or provided with a relatively high confining pressure. Compression failure occurs in columns subjected to a relatively high axial load level and/or provided with a relatively low confining pressure. In between these two failure modes, balanced failure occurs in columns subjected to a moderate axial load level and provided with a moderate confining pressure.

The axial load level at which balanced failure occurs is called the balanced axial load level and denoted by $(P/A_g f_{co})_b$. It may be rigorously evaluated using nonlinear moment-curvature analysis by an iterative process of adjusting the axial load level until balanced failure occurs. The balanced axial load levels so evaluated for column sections with concrete strength f_{co} ranging from 40 to 100 MPa, confining pressure f_r ranging from 0 to 4 MPa and longitudinal steel ratio ρ ranging from 2 to 6% are listed in Table 2. From the tabulated results, it can be seen that the balanced axial load level is not sensitive to the longitudinal steel ratio. Hence, for simplicity, the effect of the longitudinal

Table 2 Balanced axial load levels

f_{co} (MPa)	f_r (MPa)	Balanced axial load level $(P/A_g f_{co})_b$			
		ρ = 2%	ρ = 4%	ρ = 6%	Adopted value
40	0	0.44	0.47	0.52	0.48
50		0.41	0.42	0.45	0.43
60		0.39	0.40	0.41	0.40
70		0.37	0.38	0.38	0.38
80		0.36	0.36	0.37	0.36
90		0.34	0.35	0.35	0.35
100		0.33	0.34	0.34	0.34
40	1	0.64	0.69	0.75	0.69
50		0.58	0.62	0.67	0.63
60		0.53	0.57	0.61	0.57
70		0.50	0.53	0.56	0.53
80		0.47	0.50	0.52	0.50
90		0.45	0.46	0.49	0.47
100		0.43	0.44	0.46	0.44
40	2	0.76	0.81	0.87	0.81
50		0.68	0.72	0.77	0.73
60		0.62	0.66	0.70	0.66
70		0.58	0.61	0.65	0.61
80		0.54	0.57	0.60	0.57
90		0.51	0.54	0.56	0.54
100		0.49	0.51	0.53	0.51
40	3	0.86	0.92	0.98	0.92
50		0.77	0.82	0.87	0.82
60		0.70	0.74	0.78	0.74
70		0.65	0.68	0.72	0.68
80		0.61	0.64	0.66	0.64
90		0.57	0.60	0.62	0.60
100		0.54	0.56	0.59	0.56
40	4	1.02	1.02	1.02	1.02
50		0.86	0.89	0.95	0.90
60		0.78	0.82	0.85	0.82
70		0.72	0.75	0.78	0.75
80		0.67	0.70	0.72	0.70
90		0.62	0.65	0.68	0.65
100		0.59	0.61	0.63	0.61

steel ratio on the balanced axial load level may be ignored and a single value of balanced axial load level may be adopted for each combination of concrete strength and confining pressure. The single value of balanced axial load level to be adopted may be taken as the average of the balanced axial load levels at ρ=2, 4 and 6%, as tabulated in the last column of Table 2.

Correlating the above rigorously evaluated balanced axial load levels to the concrete strength and confining pressure, the following formula for direct evaluation of the balanced axial load level is derived:

$$(P/A_g f_{co})_b = 3.1(f_{co})^{-0.5}(1+2f_r)^{0.3} \tag{1}$$

This formula is generally accurate to within 10% errors, which should be sufficiently good for practical design applications.

3.2 Flexural ductility analysis

The flexural ductility of columns is expressed in terms of curvature ductility factor defined by Park and Paulay (1975) as:

$$\mu = \phi_u/\phi_y \tag{2}$$

where μ=curvature ductility factor, ϕ_u=ultimate curvature and ϕ_y=yield curvature. The ultimate curvature ϕ_u is taken as the curvature when the resisting moment has after reaching the peak moment M_p dropped to 0.8 M_p, while the yield curvature ϕ_y is taken as that of an equivalent linearly elastic-perfectly plastic system, which is actually equal to 4/3 times the curvature at 0.75 M_p before reaching the peak moment. The definitions of yield and ultimate curvatures are illustrated in Fig. 4.

The curvature ductility factors are plotted against the various parameters at different confining pressures in Fig. 5. Fig. 5(a) shows the variation of the curvature ductility factor μ with the concrete strength f_{co}. It is seen that at a constant confining pressure, the flexural ductility gradually decreases as the concrete strength increases. This indicates that if HSC columns are designed just like NSC columns, the flexural ductility would tend to be relatively low. It is also seen that at a higher

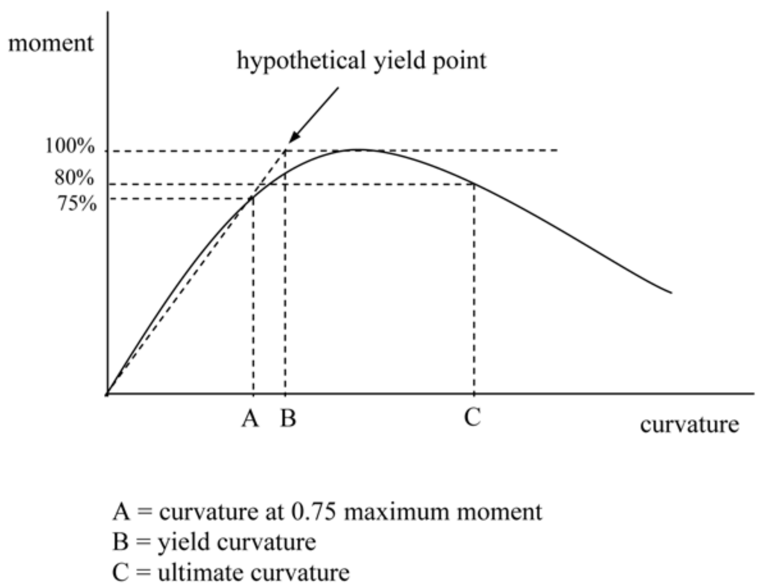

Fig. 4 Definitions of yield and ultimate curvatures

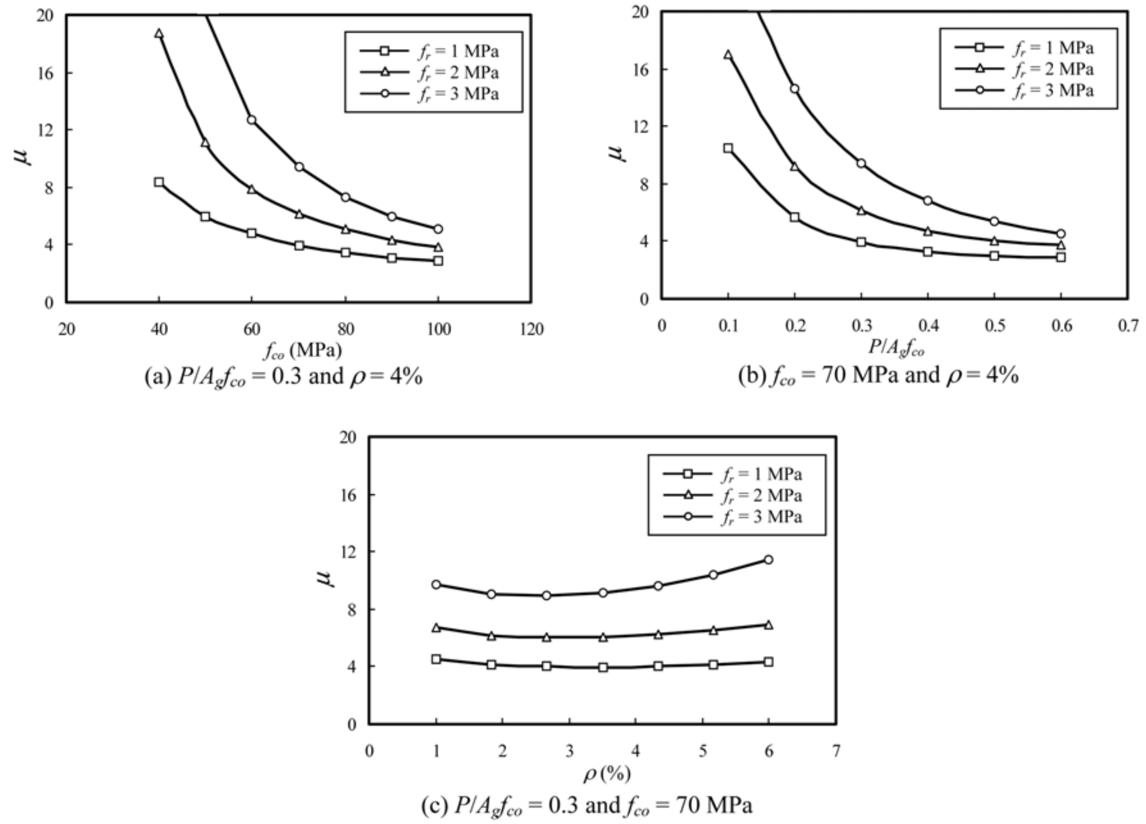

Fig. 5 Effect of concrete strength, axial load level and longitudinal steel ratio on ductility

confining pressure, the flexural ductility is generally higher. Hence, the reduction in flexural ductility due to the use of HSC instead of NSC may be replenished by increasing the confining pressure. Fig. 5(b) shows the variation of the curvature ductility factor μ with the axial load level $P/A_g f_{co}$. It is noted that at a constant confining pressure, the flexural ductility rapidly decreases as the axial load level increases. Therefore, if no limit is imposed on the maximum axial load level, the flexural ductility might become unacceptably low. As before, since the provision of a higher confining pressure would increase flexural ductility, the adverse effect of a higher axial load level may be counteracted by providing a higher confining pressure. Fig. 5(c) shows the variation of the curvature ductility factor μ with the longitudinal steel ratio ρ. It is obvious from this figure that regardless of the confining pressure provided, the flexural ductility is not sensitive to the longitudinal steel ratio.

From the above, it is evident that the flexural ductility of a column decreases as the concrete strength or the axial load level increases but increases as the confining pressure increases. Furthermore, to avoid the flexural ductility from becoming unacceptably low, an upper limit should be imposed on the maximum axial load level. Alternatively, in order to restore the flexural ductility to an acceptable level, a lower limit should be imposed on the minimum confining pressure. In other words, to ensure the achievement of a certain minimum flexural ductility, it is necessary to limit either the maximum axial load level or the minimum confining pressure.

3.3 Minimum flexural ductility requirement

In the existing design codes, just barely minimum confining reinforcement is provided to the concrete columns unless they are required to resist impact or earthquake loads. In fact, the confining reinforcement is provided primarily to restrain outward buckling of the longitudinal reinforcement. Consequently, as explained before and listed in Table 1, the confining pressure provided is only about 0.2 MPa. With such a fixed confining pressure provided, the curvature ductility factor is not really consistent. Within the range of concrete strength f_{co} from 20 to 40 MPa and the range of axial load level $P/A_g f_{co}$ from 0.2 to 0.4, the actual curvature ductility factor achieved could vary between 2.73 to 6.00, as presented in Table 1. On the whole, provided the concrete strength f_{co} is not higher than 40 MPa and the axial load level $P/A_g f_{co}$ is not higher than 0.4, an average curvature ductility factor of 4.46 and a minimum curvature ductility factor of 2.80 are provided. In order to provide a consistent level of nominal flexural ductility, it is advocated that instead of imposing empirical deemed-to-satisfy detailing rules or imposing a fixed minimum confining pressure, the nominal requirement should be set by imposing a fixed minimum curvature ductility factor μ_{min}. As the minimum curvature ductility factor being provided to concrete beams is 3.32 (Ho *et al.* 2004), it is proposed that this same minimum ductility should be provided to concrete columns, which, from the robustness point of view, are key structural elements.

With a fixed minimum curvature ductility factor μ_{min} set as nominal requirement, certain limits are automatically imposed on the various design parameters, which govern the flexural ductility of concrete columns. From Fig. 5(a), it can be seen that for a given combination of axial load level and confining pressure, there is a maximum concrete strength at which the required μ_{min} is just achieved. However, as the concrete strength is usually prescribed at the schematic design stage and a HSC is used to take advantage of its higher strength, it is not considered advisable to impose any unnecessarily restrictive limit on the concrete strength. Instead, since the flexural ductility decreases with increasing axial load level and increases with increasing confining pressure, as depicted in Fig. 5(b), a limit should be imposed on either the maximum axial load level $(P/A_g f_{co})_{max}$ or the minimum confining pressure $(f_r)_{min}$. However, since the flexural ductility is dependent on both the axial load level and confining pressure, the limits to be imposed cannot be set as constant values. Lastly, since the flexural ductility is not sensitive to the longitudinal steel ratio, as shown in Fig. 5(c), it should be simpler to impose limits on the maximum axial load level or minimum confining pressure that are independent of the longitudinal steel ratio but applicable to a broad range of longitudinal steel ratios.

4. Maximum axial load level

For any given set of concrete strength f_{co}, confining pressure f_r and longitudinal steel ratio ρ, the maximum axial load level $(P/A_g f_{co})_{max}$ for achieving a minimum curvature ductility factor of μ_{min} = 3.32 can be evaluated using nonlinear moment-curvature analysis by an iterative method of successively adjusting the axial load level $P/A_g f_{co}$ until the curvature ductility factor μ is equal to 3.32. The values of $(P/A_g f_{co})_{max}$ so obtained for different combinations of concrete strength, confining pressure and longitudinal steel ratio are presented in Table 3.

From the table, it is evident that the maximum axial load level decreases as the concrete strength increases but increases as the confining pressure increases. Hence, when HSC is used in place of NSC with no increase in the confining pressure, the maximum axial load level has to be reduced,

Table 3 Maximum axial load levels

f_{co} (MPa)	f_r (MPa)	Maximum axial load level $(P/A_g f_{co})_{max}$			
		$\rho = 2\%$	$\rho = 4\%$	$\rho = 6\%$	Adopted value
40	0	0.26	0.27	0.31	0.26
50		0.21	0.20	0.22	0.20
60		0.18	0.16	0.16	0.16
70		0.16	0.13	0.12	0.12
80		0.15	0.12	0.10	0.10
90		0.14	0.11	0.09	0.09
100		0.13	0.10	0.08	0.08
40	0.5	0.56	0.60	0.65	0.56
50		0.35	0.39	0.41	0.35
60		0.32	0.34	0.35	0.32
70		0.27	0.30	0.32	0.27
80		0.27	0.27	0.28	0.27
90		0.23	0.25	0.27	0.23
100		0.22	0.23	0.23	0.22
40	1	0.75	0.90	> 1.0	0.75
50		0.62	0.72	0.85	0.62
60		0.53	0.59	0.68	0.53
70		0.44	0.39	0.46	0.39
80		0.34	0.32	0.33	0.32
90		0.31	0.29	0.29	0.29
100		0.28	0.26	0.26	0.26
40	2	0.97	> 1.0	> 1.0	0.97
50		0.82	0.95	> 1.0	0.82
60		0.71	0.81	> 1.0	0.71
70		0.63	0.70	0.78	0.63
80		0.57	0.62	0.68	0.57
90		0.50	0.54	0.57	0.50
100		0.44	0.43	0.42	0.42
40	3	> 1.0	> 1.0	> 1.0	> 1.0
50		0.97	> 1.0	> 1.0	0.97
60		0.86	0.96	> 1.0	0.86
70		0.76	0.84	0.95	0.76
80		0.68	0.75	0.82	0.68
90		0.61	0.66	0.72	0.61
100		0.56	0.60	0.64	0.56
40	4	> 1.0	> 1.0	> 1.0	> 1.0
50		> 1.0	> 1.0	> 1.0	> 1.0
60		0.94	> 1.0	> 1.0	0.94
70		0.85	0.93	> 1.0	0.85
80		0.77	0.84	0.92	0.77
90		0.70	0.75	0.82	0.70
100		0.63	0.68	0.74	0.63

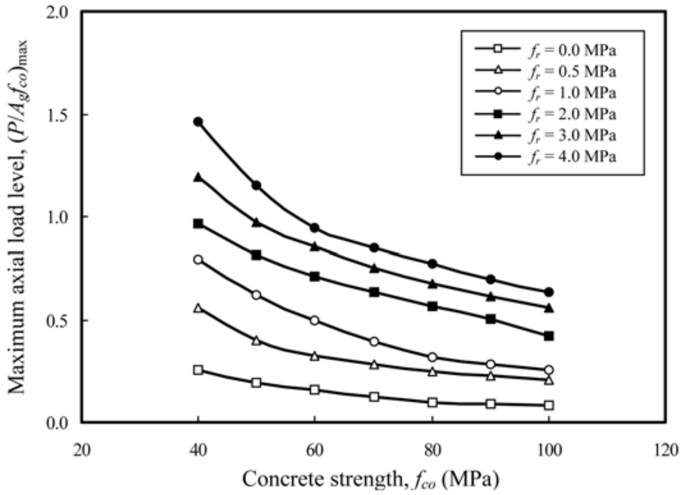

Fig. 6 Maximum axial load level plotted against concrete strength

thus restricting the beneficial use of HSC. Nevertheless, with the confining pressure increased, the maximum axial load level may be increased to allow better use of the HSC. From the maximum axial load levels at different longitudinal steel ratios, it is also evident that the maximum axial load level varies only slightly with the longitudinal steel ratio. Hence, for simplicity, the effect of the longitudinal steel ratio may be ignored and a single value of maximum axial load level may be adopted for each combination of concrete strength and confining pressure. The single value to be adopted is taken as the lower bound of the maximum axial load levels at ρ=2, 4 and 6%, as tabulated in the last column of Table 3. These maximum axial load levels, which are independent of the longitudinal steel ratio, should be applicable within the range of longitudinal steel ratio $\rho \leq 6\%$.

The values of $(P/A_g f_{co})_{max}$ tabulated in the last column of Table 3 are plotted against the concrete strength f_{co} for different values of confining pressure f_r in Fig. 6. It is noted that for unconfined columns, the maximum axial load levels are generally very low (≤ 0.26 for $f_{co} \geq 40$ MPa). With the provision of some confinement amounting to just f_r=0.5 MPa, the maximum axial load levels would increase dramatically by up to or even more than 100%. Hence, at least some confinement should always be provided or otherwise the maximum axial load level would be too low to allow effective use of the strength potential of the concrete.

5. Minimum confining pressure

Likewise, for any given set of concrete strength f_{co}, axial load level $P/A_g f_{co}$ and longitudinal steel ratio ρ, the minimum confining pressure $(f_r)_{min}$ for achieving a minimum curvature ductility factor of μ_{min}=3.32 can be evaluated using nonlinear moment-curvature analysis by an iterative method of successively adjusting the confining pressure f_r until the curvature ductility factor μ is equal to 3.32. The values of $(f_r)_{min}$ so obtained for different combinations of concrete strength, axial load level and longitudinal steel ratio are presented in Table 4.

From the table, it is seen that the minimum confining pressure increases as the concrete strength or the axial load level increases. Hence, when HSC is used in place of NSC or the column is heavily

Table 4 Minimum confining pressures

f_{co} (MPa)	$(P/A_g f_{co})$	Minimum confining pressure $(f_r)_{min}$			
		ρ = 2%	ρ = 4%	ρ = 6%	Adopted value
40	0.1	0.00	0.00	0.00	0.00
50		0.00	0.00	0.00	0.00
60		0.00	0.00	0.00	0.00
70		0.00	0.00	0.00	0.00
80		0.00	0.00	0.00	0.00
90		0.00	0.00	0.02	0.02
100		0.00	0.00	0.07	0.07
40	0.2	0.00	0.00	0.00	0.00
50		0.00	0.00	0.00	0.00
60		0.01	0.02	0.02	0.02
70		0.03	0.06	0.09	0.09
80		0.06	0.13	0.20	0.20
90		0.14	0.24	0.34	0.34
100		0.24	0.36	0.46	0.46
40	0.3	0.06	0.03	0.00	0.06
50		0.23	0.16	0.08	0.23
60		0.39	0.32	0.27	0.39
70		0.57	0.56	0.51	0.57
80		0.71	0.70	0.78	0.78
90		0.95	1.01	1.07	1.07
100		1.22	1.23	1.35	1.35
40	0.4	0.30	0.22	0.11	0.30
50		0.52	0.42	0.35	0.52
60		0.73	0.70	0.62	0.73
70		0.95	0.91	0.92	0.95
80		1.20	1.15	1.18	1.20
90		1.51	1.39	1.50	1.51
100		1.83	1.84	1.85	1.85
40	0.5	0.39	0.26	0.12	0.39
50		0.68	0.52	0.41	0.68
60		1.00	0.84	0.70	1.00
70		1.34	1.17	0.99	1.34
80		1.68	1.54	1.35	1.68
90		2.02	1.84	1.78	2.02
100		2.47	2.25	2.20	2.47
40	0.6	0.50	0.31	0.17	0.50
50		0.98	0.73	0.46	0.98
60		1.43	1.09	0.78	1.43
70		1.88	1.52	1.12	1.88
80		2.27	1.89	1.56	2.27
90		2.89	2.56	2.12	2.89
100		3.47	3.13	2.80	3.47

Note: f_r=$0.5k_e\rho_s f_{yh}$, where ρ_s and f_{yh} are the volumetric ratio and yield strength of confinement respectively; k_e is the confinement effectiveness factor defined by Mander *et al.* (1988).

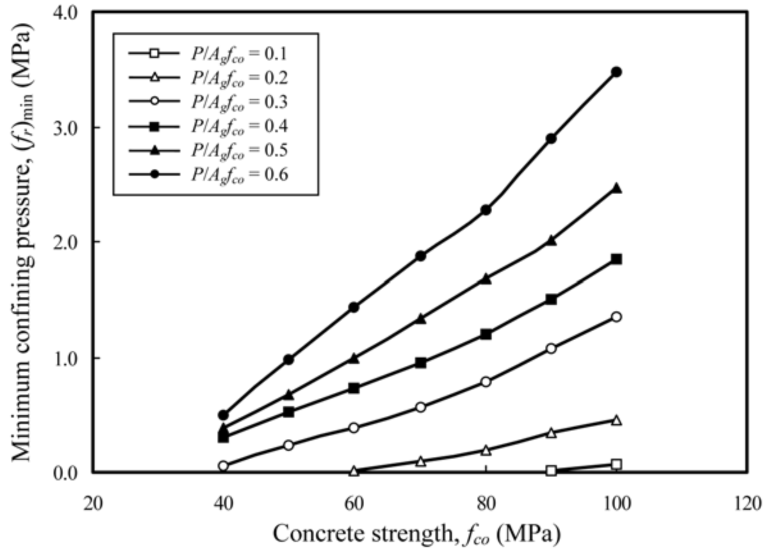

Fig. 7 Minimum confining pressure plotted against concrete strength

loaded, a higher confining pressure needs to be provided. From the minimum confining pressures at different longitudinal steel ratios, it is also seen that the minimum confining pressure varies only slightly with the longitudinal steel ratio. Hence, for simplicity, the effect of the longitudinal steel ratio may be ignored and a single value of minimum confining pressure may be adopted for each combination of concrete strength and axial load level. The single value to be adopted is taken as the upper bound of the minimum confining pressures at ρ=2, 4 and 6%, as tabulated in the last column of Table 4. These minimum confining pressures, which are independent of the longitudinal steel ratio, should be applicable within the range of longitudinal steel ratio $\rho \leq 6\%$.

The values of $(f_r)_{\min}$ tabulated in the last column of Table 4 are plotted against the concrete strength f_{co} for different values of axial load level $P/A_g f_{co}$ in Fig. 7. It is noted that the rate of increase of $(f_r)_{\min}$ with respect to $(P/A_g f_{co})$ is generally higher at a higher concrete strength. For example, if the axial load level is increased from 0.3 to 0.6, then at f_{co}=40 MPa, the value of $(f_r)_{\min}$ would increase by 0.44 MPa (from 0.06 to 0.50 MPa) while at f_{co}=80 MPa, the value of $(f_r)_{\min}$ would increase by 1.49 MPa (from 0.78 to 2.27 MPa). This indicates the effectiveness of the confining pressure or reinforcement is lower at a higher concrete strength. Hence, the empirical rules in the existing design codes, which were originally developed for application to NSC columns, must not be extrapolated for application to HSC columns.

6. Design formulas and chart

The maximum axial load level and minimum confining pressure for any given combination of design parameters may be rigorously evaluated using nonlinear moment-curvature analysis. However, such nonlinear analysis is rather cumbersome and not really practical. To resolve this problem, design formulas for direct evaluation of the maximum axial load level and minimum confining pressure are developed in the following for practical design applications.

Correlating the maximum axial load levels listed in the last column of Table 3 (values of $(P/A_g f_{co})_{\max} > 1.0$ or < 0.1 are ignored because they fall outside the practical range) to the respective concrete strengths and confining pressures, the following formula for direct evaluation of the maximum axial load level is derived:

$$(P/A_g f_{co})_{\max} = 24.5(f_{co})^{-1.20}(1+3.5f_r)^{0.65} \tag{3}$$

Comparing the predicted values by the above formula to the rigorously evaluated values by nonlinear moment-curvature analysis, it can be shown that the predicted values of maximum axial load level are generally accurate to within an error of 17%. Hence, this formula should be sufficiently accurate for practical applications.

Similarly, correlating the minimum confining pressures listed in the last column of Table 4 (values of $(f_r)_{\min}$<0.2 MPa are ignored because they fall outside the practical range) to the respective concrete strengths and axial load levels, the following formula for direct evaluation of the minimum confining pressure is derived:

$$(f_r)_{\min} = 0.0019(f_{co})^{1.85}(P/A_g f_{co})^{1.54} - 0.28 \tag{4}$$

Comparing the predicted values by the above formula to the rigorously evaluated values by nonlinear moment-curvature analysis, it can be shown that the predicted values of minimum confining pressure are generally accurate to within an error of 17%. Hence, this formula should also be acceptable for practical applications.

Putting Eqs. (3) and (4) together, it can be seen that they are equivalent to each other, in the sense that that Eq. (4) can be derived by solving Eq. (3) for the minimum confining pressure while Eq. (3) can be derived by solving Eq. (4) for the maximum axial load level. Combining these two equations, the following equation is obtained as the condition for achieving the required minimum curvature ductility factor of $\mu_{\min}$=3.32:

$$\frac{(P/A_g f_{co})}{(1+3.5f_r)^{0.65}} \le 24.5(f_{co})^{-1.20} \tag{5}$$

This equation reveals that for any prescribed concrete strength, there are many possible combinations of limiting values of axial load level and confining pressure that would lead to the achievement of the required minimum flexural ductility. These combinations are best studied by plotting the corresponding values of axial load level and confining pressure calculated by Eq. (5) in the form of contour lines for different concrete strengths in an interaction diagram, as shown in Fig. 8. It is noteworthy that the area underneath the contour line for a prescribed concrete strength demarcates the scenario of $\mu > \mu_{\min}$ whereas the area above the contour line demarcates the scenario of $\mu < \mu_{\min}$. This figure may be used as a design chart for determining the desirable combination of axial load level and confining pressure for achieving the required minimum flexural ductility. Although Figs. 6 and 7 may also be used as design charts, Fig. 8 should be more convenient to use because very often both the axial load level and the confining pressure need to be considered at the same time during the design process.

Based on Fig. 8, the role of the failure mode in the ductility design of concrete columns may be revealed by expressing the maximum axial load level in terms of the axial load to balanced axial load ratio, which is denoted by γ and defined by:

$$\gamma = (P/A_g f_{co})/(P/A_g f_{co})_b \tag{6}$$

When $\gamma < 1.0$, tension failure occurs and when $\gamma > 1.0$, compression failure occurs. In general, the

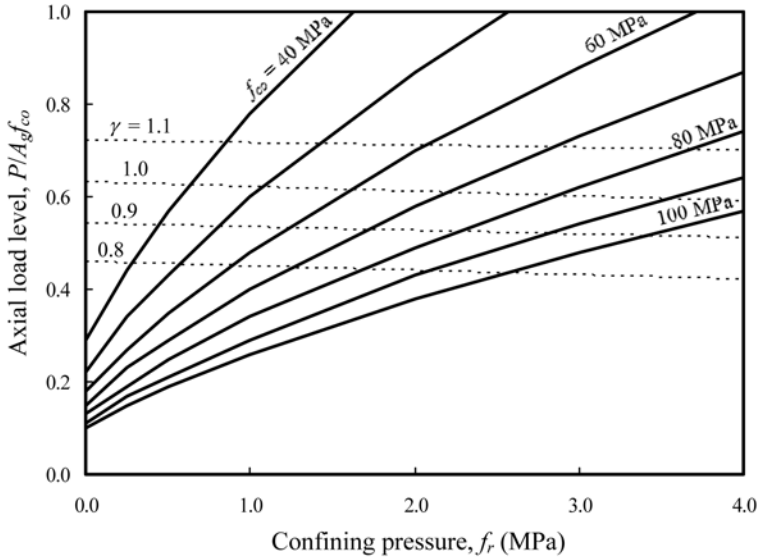

Fig. 8 Design chart for axial load level and confining pressure

flexural ductility is higher when tension failure occurs and is lower when compression failure occurs. There is a common belief among structural engineers that sufficient nominal flexural ductility may be provided to concrete columns simply by allowing only tension failure to occur, as in the case of concrete beams. To investigate whether this belief is correct, in Fig. 8, the contours of γ = 1.1, 1.0, 0.9 and 0.8 are also plotted. It should be noted that the area underneath the contour line γ = 1.0 denotes the occurrence of tension failure whereas the area above the contour line denotes the occurrence of compression failure.

From these contour lines, it can be seen that the failure mode has no direct bearing on whether the required $\mu_{\min}$ would be achieved. When the concrete strength is high and/or the confining pressure is low, the occurrence of tension failure does not guarantee the achievement of $\mu_{\min}$. For example, for a column with f_{co}=80 MPa and f_r=1 MPa, and subjected to $P/A_g f_{co}$=0.45, tension failure would occur but the required $\mu_{\min}$ would not be achieved. On the other hand, when the concrete strength is low and/or the confining pressure is high, the occurrence of compression failure does not necessarily hinder the achievement of $\mu_{\min}$. For example, for a column with f_{co}=60 MPa and f_r=2 MPa, and subjected to $P/A_g f_{co}$=0.70, compression failure would occur but the required $\mu_{\min}$ would be achieved. Hence, controlling the failure mode is not a proper way of ensuring the achievement of the required minimum flexural ductility.

7. Existing design codes

In the existing design codes (ACI Committee 318 2005, Buildings Department 2004, European Committee for Standardization 2002, Ministry of Construction 2002, Standard Australia 2001), only empirical rules for the detailing of the confining reinforcement are imposed, which, as depicted in Table 1, are equivalent to the provision of a nominal confining pressure of about 0.2 MPa. Most of the design codes do not impose any limit on the maximum axial load level. However, since the flexural ductility would decrease as the axial load level increases, the maximum axial load level should be controlled or otherwise the flexural ductility could become unacceptably low. Substituting the confining pressure of 0.2 MPa into Eq. (3), the maximum axial load level to be imposed in conjunction with the empirical detailing rules in the existing design codes is obtained as:

$$(P/A_g f_{co})_{\max} = 34.6(f_{co})^{-1.20} \tag{7}$$

For NSC columns with $f_{co} \leq 40$ MPa, the maximum axial load level is 0.41. However, for HSC columns, the maximum axial load level would decrease to 0.25 at f_{co}=60 MPa, 0.18 at f_{co}=80 MPa, and 0.14 at f_{co}=100 MPa. These maximum axial load levels are much too low for the effective use of HSC. Hence, it is professed that the empirical detailing rules in the existing design codes are not applicable to HSC columns and that even when these empirical rules are applied to NSC columns, an additional requirement of limiting the maximum axial load level at 0.4 should be imposed.

If the same maximum axial load level of 0.4 were to be applied in the design of HSC columns, the confining pressure has to be increased. Substituting the axial load level of 0.4 into Eq. (4), the minimum confining pressure needed is obtained as:

$$(f_r)_{\min} = 0.0005(f_{co})^{1.85} - 0.28 \tag{8}$$

For NSC columns with $f_{co} \leq 40$ MPa, the minimum confining pressure is 0.2 MPa. But, for HSC columns, the minimum confining pressure has to be increased to 0.69 MPa at f_{co}=60 MPa, 1.38 MPa at f_{co}=80 MPa, and 2.23 MPa at f_{co}=100 MPa. Hence, if the existing design codes were to be applied to HSC columns with the same maximum axial load level of 0.4 imposed, the rules for the detailing of confining reinforcement have to be changed to cater for the above minimum confining pressure requirements.

Although the existing design codes do allow the use of HSC, so far very few guidelines have been provided for the ductility design of HSC members. This is unsafe as the use of HSC without proper detailing or with no limitations imposed could lead to insufficient ductility or even brittle failure. It is advocated that as HSC is becoming more and more commonly used, it is now a matter of urgency to incorporate some ductility design rules in the design codes. For concrete beams, the minimum ductility design method developed in a previous study by the authors (Ho *et al.* 2004) may be referred to while for concrete columns, the ductility design method developed in the present study should be a useful reference.

8. Conclusions

The empirical deemed-to-satisfy detailing rules for concrete columns in the existing design codes have been reviewed. It was found by theoretical analysis that the confining pressure being provided is rather low and that the curvature ductility factor so achieved is not consistent, being generally lower at higher concrete strength or higher axial load level. Therefore, when these empirical rules are applied to HSC columns or heavily loaded columns, the flexural ductility could become unacceptably low. It is thus advocated that these empirical rules in the existing design codes should be changed or even better replaced by a more scientific approach of requiring a minimum curvature ductility factor $\mu_{\min}$ to be achieved. As the value of $\mu_{\min}$ being provided by the existing design codes to NSC beams and columns is around 3.32, it is suggested to set $\mu_{\min}$=3.32 as a nominal requirement for all members, including HSC beams and columns, except for members subjected to impact or earthquake loads, in which case, the value of $\mu_{\min}$ should be increased to meet with the actual ductility demand.

Using nonlinear moment-curvature analysis, the effects of the concrete strength, axial load level, confining pressure and longitudinal steel ratio on the flexural ductility of concrete columns have been studied. The analytical results revealed that the flexural ductility decreases as the concrete strength or the axial load level increases, increases as the confining pressure increases, and is not sensitive to the longitudinal steel ratio. Based on these results, a set of maximum axial load levels and a set of minimum confining pressures for achieving the minimum curvature ductility factor of $\mu_{\min}$=3.32 have been obtained. As the maximum axial load level is dependent on the confining pressure and the minimum confining pressure is dependent on the axial load level, no single limit could be imposed on either the maximum axial load level or the minimum confining pressure. Nevertheless, by correlation analysis, one formula for evaluating the maximum axial load level in terms of the concrete strength and confining pressure and another formula for evaluating the minimum confining pressure in terms of the concrete strength and axial load level have been derived. Both formulas are applicable to the range of longitudinal steel ratio not higher than 6%. Furthermore, a design chart for evaluating the allowable combinations of axial load level and confining pressure at any given concrete strength ranging from NSC to HSC has been produced.

Finally, it is proposed that if the empirical detailing rules in the existing design codes were to be retained, a maximum axial load level which decreases with the concrete strength as per Eq. (7) should be imposed and that if the maximum axial load level is set as a constant of 0.4, a minimum confining pressure which increases with the concrete strength as per Eq. (8) should be imposed.

References

ACI Committee 318 (2005), *Building Code Requirements for Reinforced Concrete and Commentary ACI 318M-05*, Manual of Concrete Practice, American Concrete Institute, Michigan, USA, 436.

Au, F.T.K and Bai, Z.Z. (2006), "Effect of axial load on flexural behaviour of cyclically loaded RC columns", *Comput. Concrete*, **3**(4), 261-284.

Au, F.T.K., Bai, Z.Z. and Kwan, A.K.H. (2005), "Complete moment-curvature relationship of reinforced normal- and high-strength concrete beams experiencing complex load histroy", *Comput. Concrete*, **2**(4), 309-324.

Au, F.T.K. and Kwan, A.K.H. (2004), "A minimum ductility design method for non-rectangular high-strength concrete beams", *Comput. Concrete*, **1**(2), 115-130.

Attard, M.M. and Setunge, S. (1996), "The stress strain relationship of confined and unconfined concrete", *ACI Mater. J.*, **93**(5), 432-442.

Bayrak, O. and Sheikh, S.A. (1997), "High strength concrete columns under simulated earthquake loading", *ACI Struct. J.*, **94**(6), 708-722.

Bayrak, O. and Sheikh, S.A. (1998), "Confinement reinforcement design consideration for ductile HSC columns", *J. Strut. Eng-ASCE*, **124**(9), 999-1010.

Bechtoula, H., Sakashita, M., Kono, S. and Watanabe, F. (2005), "Seismic performance of 1/4-scale RC frames subjected to axial and cyclic reversed lateral loads", *Comput. Concrete*, **2**(2), 147-164.

Buildings Department (2004), *Code of Practice for Structural Use of Concrete 2004*, The Government of Hong Kong Special Administrative Region, 180.

Carreira, D.J. and Chu, K.H. (1986), "The moment-curvature relationship of reinforced concrete members", *ACI ACE J. Proceed.*, **83**(2), 191-198.

Chung, Y.S., Park, C.K. and Lee, E.H. (2004), "Seismic performance and damage assessment of reinforced concrete bridge piers with lap-spliced longitudinal steels", *Struct. Eng. Mech.*, **17**(1), 99-112.

Chung, Y.S., Park, C.K. and Lee, D.H. (2006), "Seismic performance of RC bridge piers subjected to moderate earthquakes", *Struct. Eng. Mech.*, **24**(4), 429-446.

European Committee for Standardization (2004), *Eurocode 2: Design of concrete structures: Part 1-1: General rules and rules for buildings*, UK, 225.

Fafitis, A. and Shah, S.P. (1985), "Prediction of ultimate behavior of confined columns subjected to large deformations" *ACE J. Proceed.*, **82**(4), 423-433.

Galal, K. (2007), "Lateral force-displacement ductility relationship of non-ductile squat RC columns rehabilitated using FRP confinement", *Struct. Eng. Mech.*, **25**(1), 75-89.

Ho, J.C.M., Kwan, A.K.H. and Pam, H.J. (2004), "Minimum flexural ductility design of high-strength concrete beams", *Mag. Concrete Res*., **56**(1), 13-22.

Ho, J.C.M., Au, F.T.K. and Kwan, A.K.H. (2005), "Effects of strain hardening of steel reinforcement on flexural strength and ductility of concrete beams", *Struct. Eng. Mech.,* **19**(2), 185-198.

Kim, J.H. (2005), "Ductility enhancement of reinforced concrete thin wall", *Comput. Concrete*, **2**(2), 111-123.

Kim, T. and Kim, J. (2007), "Seismic performance evaluation of a RC special moment frame", *Struct. Eng. Mech.*, **27**(6), 671-682.

Kim, T.H., Park, J.G., Kim, Y.J. and Shin, H.M. (2008), "A computation platform for seismic performance assessment of reinforced concrete bridge piers with unbonded reinforcing or prestressing bars", *Comput. Concrete*, **5**(2), 135-154.

Kwan, A.K.H., Ho, J.C.M. and Pam, H.J. (2002), "Flexural strength and ductility of reinforced concrete beams", *P. I. Civil Eng-Str. B.*, **152**(4), 361-369.

Kwan, A.K.H., Au, F.T.K. and Chau, S.L. (2004), "Theoretical study on effect of confinement on flexural ductility of normal and high-strength concrete beams", *Mag. Concrete Res*., **56**(5), 299-309.

Li, B., Park, R. and Tanaka, H. (1991), "Effect of confinement on the behaviour of high strength concrete columns under seismic loading", *Proceedings of the 5th Pacific Conference on Earthquake Engineering*, Auckland, November.

Lu, X. and Zhou, Y. (2007), "An applied model for steel reinforced concrete columns", *Struct. Eng. Mech.*, **27**(6), 697-711.

Maghsoudi, A.A. and Bengar, H.A. (2006), "Flexural ductility of HSC members", *Struct. Eng. Mech.*, **24**(2), 195-212.

Mander, J.B., Priestley, M.J.N. and Park, R. (1988), "Theoretical stress-strain model for confined concrete", *J. Struct. Eng-ASCE*, **114**(8), 1804-1825.

Marefat, M.S., Khanmohammadi, M., Bahrani, M.K. and Goli, A. (2005), "Cyclic load testing and numerical modelling of concrete columns with substandard seismic details", *Comput. Concrete*, **2**(5), 367-380.

Mendis, P.A., Kovacic, D. and Setunge, S. (2000), "Basis for the design of lateral reinforcement for high-strength concrete columns", *Struct. Eng. Mech.*, **9**(6), 589-600.

Ministry of Construction (2002), *Code for Design of Concrete Structures GB 50010-2002*, People's Republic of China, 96.

Park, R. and Paulay, T. (1975), *Reinforced Concrete Structures*, Wiley, New York, U.S.A., 769.

Razvi, S.R. and Saatcioglu, M. (1994), "Strength and deformability of confined high-strength concrete columns", *ACI Struct. J.*, **91**(6), 1-10.

Rubinstein, M., Moller, O. and Giuliano, A. (2007), "Preliminary design and inelastic assessment of earthquake-resistant structural systems", *Struct. Eng. Mech.*, **26**(3), 297-313.

Sheikh, S.A., Shah, D.V. and Khoury, S.S. (1994), "Confinement of high-strength concrete columns", *ACI Struct. J.*, **91**(1), 100-111.

Sung, Y.C., Liu, K.Y., Su, C.K., Tsai, I.C. and Chang, K.C. (2005), "A study on pushover analyses of reinforced concrete columns", *Struct. Eng. Mech.*, **21**(1), 35-52.

Standard Australia (2001), *Australian Standard Concrete Structures AS 3600-2001*, Australia, 175.

Watson, S. and Park, R. (1994), "Simulated seismic load tests on reinforced concrete columns", *J. Struct. Eng-ASCE,* **120**(6), 1825-1849.

Wu, Y.F., Oehlers, D.J. and Griffith, M.C. (2004), "Rational definition of the flexural deformation capacity of RC column sections", *Eng. Struct.*, **26**, 641-650.

CC

Notations

A_g	Area of column section ($A_g = bh$)
A_s	Total area of longitudinal steel reinforcement
b	Breadth of column section
d	Effective depth of column section
d_b	Diameter of longitudinal reinforcement
d_i	Depth to centroid of steel at i^{th} layer from extreme compressive fibre
d_n	Depth to neutral axis
d_s	Diameter of confining reinforcement
E_s	Elastic modulus of steel reinforcement
f_{co}	Peak stress on stress-strain curve of unconfined concrete
f_r	Confining pressure produced by confining reinforcement
$(f_r)_{\min}$	Minimum confining pressure to achieve minimum curvature ductility factor
f_y	Yield strength of steel reinforcement
h	Total depth of the column section
M_p	Peak moment
P	Axial load applied at centroid
$(P/A_g f_{co})_b$	Balanced axial load level
$(P/A_g f_{co})_{\max}$	Maximum axial load level to achieve minimum curvature ductility factor
s	Spacing of confining reinforcement
γ	Axial load to balanced axial load ratio
ε_{ps}	Residual plastic strain in steel reinforcement
ε_s	Strain in steel
ϕ_u	Ultimate curvature
ϕ_y	Yield curvature
μ	Curvature ductility factor
$\mu_{\min}$	Minimum curvature ductility factor
ρ	Longitudinal steel ratio ($\rho = A_s/A_g$)
σ_s	Stress in steel reinforcement